Journal of Molecular Graphics and Modelling 75 (2017) 189–198

Contents lists available at ScienceDirect

Journal of Molecular Graphics and Modelling

journal homepage: www.elsevier.com/locate/JMGM

Topical Perspectives

Structural basis for the potent inhibition of the HIV integrase-LEDGF/p75 protein–protein interaction

Sergio R. Ribone [a,b], Mario A. Quevedo [b,*]

[a] Instituto de Investigaciones en Fisicoquímica de Córdoba (INFIQC, CONICET), Dpto. Química Orgánica, Fac. Ciencias Químicas, Universidad Nacional de Córdoba, Córdoba, X5000HUA, Argentina
[b] Unidad de Investigación y Desarrollo en Tecnología Farmacéutica (UNITEFA, CONICET), Dpto. Farmacia, Fac. Ciencias Químicas, Universidad Nacional de Córdoba, Córdoba, X5000HUA, Argentina

ARTICLE INFO

Article history:
Received 31 March 2017
Received in revised form 23 May 2017
Accepted 24 May 2017
Available online 26 May 2017

Keywords:
Anti-HIV
Inhibitors
Molecular docking
Molecular dynamics
Protein–protein interaction

ABSTRACT

Integrase (IN) constitutes one of the key enzymes involved in the lifecycle of the Human Immunodeficiency Virus (HIV), the etiological agent of AIDS. The biological role of IN strongly depends on the recognition and binding of cellular cofactors belonging to the infected host cell. Thus, the inhibition of the protein–protein interaction (PPI) between IN and cellular cofactors has been envisioned as a promising therapeutic target. In the present work we explore a structure-activity relationship for a set of 14 compounds reported as inhibitors of the PPI between IN and the lens epithelium-derived growth factor (LEDGF/p75). Our results demonstrate that the possibility to adopt the bioactive conformation capable of interacting with the hotspots IN-LEDGF/p75 hotspots residues constitutes a critical feature to obtain a potent inhibition. A ligand efficiency (|*Lig-Eff*|) quantitative descriptor combining both interaction energetics and conformational requirements was developed and correlated with the reported biological activity. Our results contribute to the rational development of IN-LEDGF/p75 interaction inhibitors providing a solid quantitative structure-activity relationship aimed for the screening of new IN-LEDGF/p75 interaction inhibitors.

1. Introduction

The advance of acquired immunodeficiency syndrome (AIDS) caused by the infection with Human Immunodeficiency Virus (HIV-1) constitutes a mayor epidemiological issue throughout the world. Although almost 30 drugs have currently being approved for the treatment of HIV-1 infection, several pharmacotherapeutic issues still represent a significant hurdle to attain efficient long-term treatments. Among those issues, the emergence of viral strains resistant to widely used anti-HIV agents constitutes one of the most urgent needs for novel research contributions. Several molecular targets involved in the HIV-1 replication cycle have been identified and validated as drug targets. Among them, HIV-1 integrase (IN) constitutes a key viral enzyme that catalyzes the processing and integration of proviral cDNA into the genome of the host cell [1,2]. This essential catalytic role constitutes an attracting therapeutic target for the design of potent and selective inhibitors [1,3].

Raltegravir (RAL) was the first IN inhibitor (INI) approved by the FDA for clinical use, and which exhibits its antiviral effect by inhibiting the catalytic activity of IN, thus hampering the integration of viral cDNA to the host cell DNA [4]. Unfortunately, upon treatment with RAL, resistant HIV strains rapidly emerge severely impairing its anti-HIV efficacy, fact that motivated the development of new INIs aimed to overcome resistance problems. In this way, second generation INIs were afterwards designed in the search of enhanced activity-resistance profiles, with dolutegravir (DTG) and elvitegravir (EVG) being approved for clinical use in 2013 and 2014, respectively [5,6]. Although the approval of these INIs constituted a major breakthrough in the antiretroviral therapy, their low genetic barrier to resistance emergence remains as an unresolved issue, and the possibility of inhibiting IN by means of alternative mechanisms was envisioned [7,8].

The integration event catalyzed by IN is a highly organized multistep process, in which several cellular cofactors are involved [7]. Among them, the lens epithelium-derived growth factor (LEDGF/p75) constitutes the first cellular protein identified as a cofactor for the integration of the viral cDNA [9]. Upon IN, LEDGF/p75 and viral cDNA interaction, a pre-integration complex (PIC) is formed in the cytoplasm, which is afterwards effectively

* Corresponding author at: Unidad de Investigación y Desarrollo en Tecnología Farmacéutica (UNITEFA, CONICET), Dpto. Farmacia, Fac. Ciencias Químicas, Universidad Nacional de Córdoba, Córdoba, X5000HUA, Argentina.
E-mail address: alfredoq@fcq.unc.edu.ar (M.A. Quevedo).

http://dx.doi.org/10.1016/j.jmgm.2017.05.019
1093-3263/

translocated to the nucleus for the final integration of the viral cDNA to the host DNA [10]. It has been vastly reported that the efficacy of IN function is significantly reduced if its binding to LEDGF/p75 is inhibited [11,12]. Thus, the development of IN-LEDGF/p75 interaction inhibitors encompasses a promising therapeutic strategy [7,11].

The design and development of protein–protein interaction (PPI) inhibitors constitutes a scientific area of emerging relevance [13,14], with an early skepticism due to the fact that PPI are typically stabilized by an extended interaction interphase, feature that may limit the possibility to modulate them by means of small molecules. Afterwards, it was observed that several PPIs are driven by a limited number of intermolecular contacts termed as "*hotspots*" [15,16]. This kind of PPIs are thus feasible of being modulated by low weight "*drug like*" organic molecules. This is the case of the IN-LEDGF/p75 interaction [17,18], with extensive proof of the concept studies supporting the observation that the interaction between these two proteins is stabilized by a limited number of interactions hotspots.

A major breakthrough towards the possibility of applying computer aided drug design techniques to the development of IN-LEDGF/p75 inhibitors was derived from the obtention of crystallographic and spectroscopic structural data of the IN catalytic core domain (IN_{CCD}) complexed with the LEDGF/p75 IN binding domain ($LEDGF_{IBD}$) (Fig. 1) [17–19]. These studies showed that the $LEDGF_{IBD}$ is formed by four α-helices (α1, α2, α4 and α5), which are connected through a pair of hairpin turns (loop1 and loop2, respectively), of which Ile365, Asp366, Phe406 and Val408 are essential for the recognition and binding to IN_{CCD} [20,21]. In counterpart, the $LEDGF_{IBD}$ binding region of IN_{CCD} is formed within the interface of two IN monomers, in which loop1 and loop2 of $LEDGF_{IBD}$ are buried upon interaction establishing stable intermolecular contacts (Fig. 1). The corresponding hotspots residues have been studied in detail in previous reports [20,21], concluding that the side chain of Ile365 in $LEDGF_{IBD}$ projects into the hydrophobic pocket formed by Thr174 and Met178 from monomer A and Leu102, Ala128, Ala129, and Trp132 from the monomer B of the $IN_{CCD.}$ In addition, residues Phe406 and Val408 of the $LEDGF_{IBD}$ interacts with Trp131 corresponding to monomer B of IN_{CCD}, while Asp366 forms stable hydrogen bond interactions with the backbone of Glu170 and His171 from monomer A of IN_{CCD} [20,21].

The proof of concept regarding the possibility to inhibit the IN-LEDGF/p75 interaction was demonstrated for the first time by Christ and Voet et. al. [22], with the development of a family of 2-(quinolin-3-yl)-acetic acid derivatives. Some of them exhibited inhibitory activities in the micromolar range as measured applying the AlphaScreen™ assay [23], while two derivatives exhibited activity in the sub-micromolar range [22]. Since then, numerous efforts towards the obtention of potent LEDGINs were reported in bibliography [24–31], including an exhaustive and detailed compilation of patents issued between 2006 and 2014 [32].

Overall, it is noteworthy that, with few exceptions, most of the LEDGINs reported to date in bibliography failed to exhibit sub-micromolar IC_{50} values despite their interaction with known hotspots residues. Several attempts to correlate LEDGINs inhibitory potencies with the corresponding intermolecular interactions are reported in bibliography [33–37], including those applying state of the art molecular modeling techniques (i.e. molecular docking, molecular dynamics and binding free energy calculations). To our knowledge, no definitive structure-activity relationship between the binding free energy derived from the intermolecular interaction of LEDGINs and their corresponding inhibitory potencies could be established, particularly for compounds in preclinical development exhibiting sub-micromolar IC_{50} values. This issue limits the possibility to raise a rational structure-activity basis regarding their inhibitory activity that may aid in the design of new IN-LEDGF/p75 interaction inhibitors, and hampers the advance of candidate molecules from the preclinical to clinical development phases.

In this context, and to make our contribution to the field, in the present work we pursued the establishment of a qualitative and quantitative structure-activity relationship to elucidate the molecular and physicochemical basis for the potent inhibition of the IN-LEDGF/p75 interaction. In this way, a model set of 14 LEDGINs previously reported in bibliography exhibiting a wide range of IC_{50} values, (i.e. including sub and supra-micromolar values), were used as a training set to elucidate at a molecular level the mode of binding, energetic interaction pattern and conformational requirements for an efficient interaction with the IN_{CCD}. To this effect, state of the art structure-based drug design techniques were applied in the search of the corresponding correlation. From the discussions and conclusions raised, it is proposed that apart from complying with the interaction with the corresponding hotspot residues, the conformational degrees of freedom related to adopting the required bioactive binding mode constitutes a key feature originating a potent (i.e. sub-micromolar) IN-LEDGF/p75 interaction inhibition. This observation is consistent with a highly pre-organized LEDGF/p75 binding site within the IN_{CCD}.

2. Materials and methods

2.1. Three dimensional structures of IN-LEDGF/p75 complexes

All the crystallographic structures were retrieve from the RCSB Protein Data Bank [38]. In the case of the IN-LEDGF/p75 complex, the dimer deposited under the PDB code: 2B4J and reported by Cherepanov et al. was used [17]. For the studies involving compounds **1-4**, the crystallographic structures deposited under the PDB codes: 3ZT1; 3ZSY; 3ZSQ; 3ZSO, respectively, were used [24]. The three dimensional structures of IN_{CCD} complexed with **5-14** were obtained by molecular docking.

2.2. Molecular docking studies

In order to perform docking assays for compounds **5-14**, the crystallographic structure deposited under the PDB code 3ZSO was used as template prior deletion of the complexed ligand. Before performing docking runs, the receptor was processed using the *Fred_Receptor* module of the *FRED3 v.3.0.0* docking software package [39]. A cubic box of 10,000 $Å^3$ was created and centered on the residue Glu170A. Standard ionization states were assumed for the residues lying within the docking box, with the shape potential grids being calculated as implemented in the software. Prior to docking assays, ligand conformer libraries were generated using the *OMEGA v.2.4.3* software developed by OpenEye Scientific Software Inc [40,41]. To generate conformer ensembles during standard docking runs, an energy window of 70 Kcal/mol was applied. Fast rigid exhaustive docking runs were performed as implemented in the *HYBRID* approach implemented in the *FRED3 v.3.0.0* docking software [39], and using the crystallographic structure of compound **4** present in PDB code 3ZSO as ligand template. The resulting docked poses were ranked using the *Chemgauss3* scoring function. Visualization and analysis of the docked poses were carried out with the *VIDA v.4.2.1* software [42]. In order to validate the docking protocols described above, ligands **1-4** were redocked on their corresponding crystallographic structures, finding RMSD values below 0.5 Å for the lowest energy docked conformation.

2.3. Molecular dynamics (MD) simulations

Starting structures intended for MD simulations were obtained either from deposited crystallographic structures (compounds **1-4**)

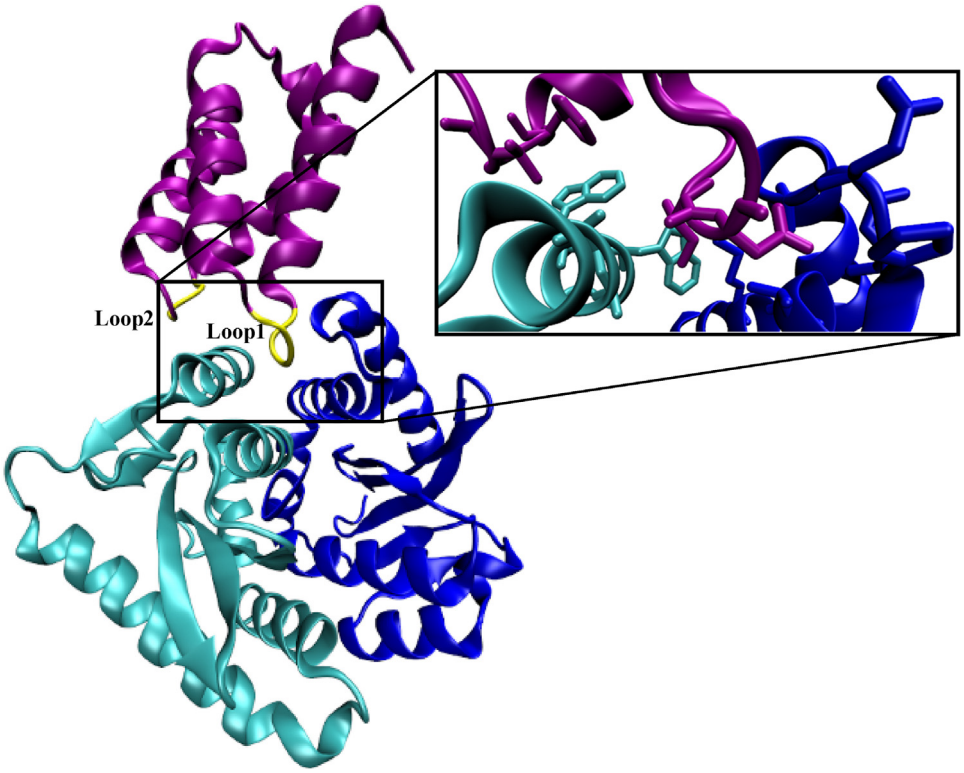

Fig. 1. Three dimensional structure of the IN-LEDGF/p75 complex binding domain as extracted from PDB code: 2B4J.

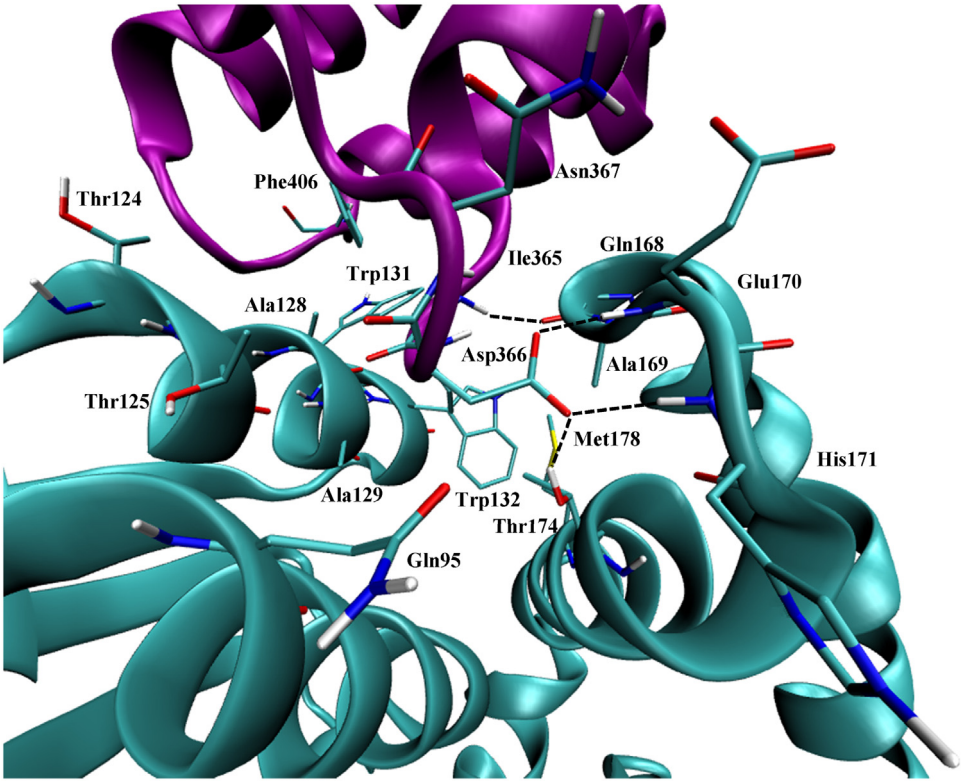

Fig. 2. Main hotspots residues interacting on the IN-LEDGF/p75 interface (INCCD is shown in cyan and LEDGF/p75 in purple). Black dotted lines indicate stable hydrogen bond interactions.

or by molecular docking (compounds **5-14**) as described in sections *2.1* and *2.2*, respectively. To perform the MD simulation of the uncomplexed IN_{CCD} and $LEDGF_{IBD}$, initial starting structures were isolated from PDB code: 2B4J. In all cases, crystallographic water molecules were removed and hydrogen atom were added using the *tLeap* module of the *Amber14* software package [43].

LEDGINs atomic charges and molecular parameters were assigned from RESP fitted charges, computed by Gaussian03 [44], and the *GAFF* force field [45], respectively, while those corresponding to IN_{CCD} were assigned based on the AMBER *ff14SB* force field [46]. The corresponding complexes were solvated using a pre-equilibrated TIP3P explicit water model, applying a solvent box with a minimum distance from the solute of 8 Å in each direction. After standard minimization procedures (5000 steps, first stage: solute restrained, second stage: unrestrained system), the minimized complexes were heated from 0 to 300 K in 0.5 ns, with restraints on the solute and constant volume conditions. Heated systems were afterwards equilibrated during 1 ns, after which the production phase at constant pressure and temperature conditions was performed for additional 30 ns, applying a time step of 2 fs. The SHAKE algorithm to constrain all covalent bonds involving hydrogen atoms was applyed. A 10 Å cutoff value was used to calculate non-bonded interactions.

In all cases, MD trajectories were obtained using CUDA designed code (*pmemd.cuda*). This work used computational resources from CCAD – Universidad Nacional de Córdoba (http://ccad.unc.edu.ar/), in particular the Mendieta Cluster, which is part of SNCAD – MinCyT, República Argentina.

2.4. Trajectory analysis and free energy of binding (MMGBSA) calculations

The *cpptraj* module of the *Amber14* [43] software package was used to analyze MD trajectories, including RMSD, *b*-factor and structural convergence analyses.

In order to quantitatively assess the free energy of binding for each ligand, the *MMPBSA.py* module was used [47]. The energy of binding was estimated by taking into account the solvation energies of the interacting molecules, in addition to the molecular mechanics (MM) energies. The contribution of polar solvation energy was computed by generalized Born (GB) implicit solvent model, while the non-polar contribution of the solvation energy was dependent on the solvent accessible surface area (SA) [48]. For the *MMGBSA* analyses, 5000 snapshots were taken from the final 25 ns of MD production.

2.5. Conformational studies

The structures of all the LEDGINs under study were subjected to exhaustive conformational analyses using the *OMEGA v.2.4.3* [40] software developed by OpenEye Scientific Software Inc. During systematic conformational searches, energy barriers from 1 to 70 kcal/mol were applied in order to evaluate the presence of the bioactive conformations. The whole set of conformer libraries were subjected to docking experiments as described above. To evaluate and confirm the presence of the bioactive conformation in each conformer library, sequential superimposition and RMSD analyses were performed. The *ShaEP* [49] software was used to superimpose the whole set of conformer libraries over the corresponding bioactive conformation obtained from the initial molecular docking experiments (Section 2.2). In a second stage, the *Obfit* module, from Open Babel chemical toolbox [50], was used to calculate the RMSD of each superimposed conformer, taking the bioactive docked conformation as reference. An RMSD value below 1 Å was assumed as positive result.

3. Results and discussion

3.1. IN-LEDGF/p75 intermolecular interaction analysis

The main objective of this initial study was to analyze the interaction hotspots involved in the stabilization of IN-LEDGF/p75 complex, studied by means of MD simulations and per-residue free energy decomposition analyses. Starting from the corresponding crystallographic complex a 30 ns MD trajectory was obtained after which MMGBSA free energy interaction analysis was performed to quantitatively assess the main interactions established between the residues of IN_{CCD} subunits and LEDGF/p75. It was observed that the total energy of binding was −40.15 kcal/mol, which is in agreement with previous studies [33,37]. A per-residue decomposition analysis was performed, identifying those residues exhibiting interaction energies below −0.75 kcal/mol. In this way it was found

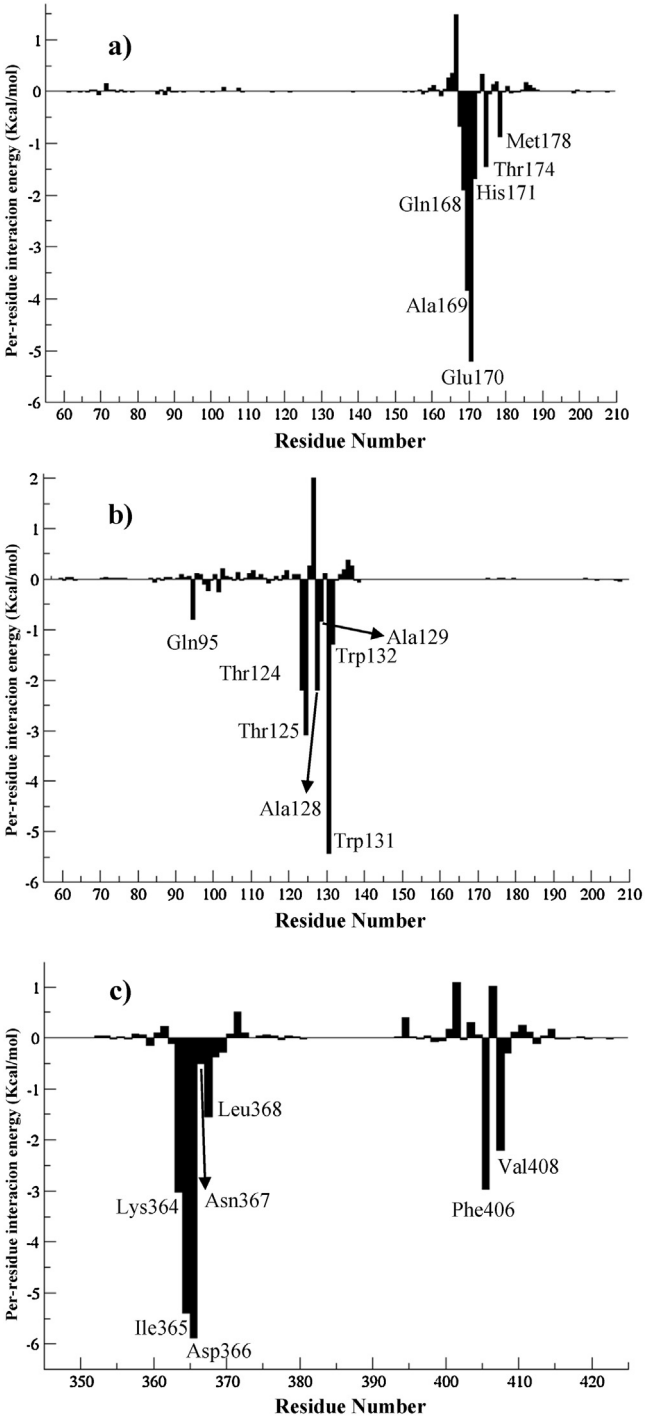

Fig. 3. Per-residue free energy decomposition analysis for the IN-LEDGF/p75 complex. a) Residues belonging to monomer A of IN_{CCD}; b) residues belonging to monomer B of IN_{CCD} and c) residues belonging to $LEDGF/p75_{IBD}$.

that Gln168, Ala169, Glu170, His171, Thr174 and Met178 from monomer A of IN_{CCD} and Gln95, Thr124, Thr125, Ala128, Ala129, Trp131, Trp132 from monomer B of the IN_{CCD} constitute the main PPI hotspots throughout the trajectory (Figs. 2 , 3 a,b). In counterpart, Lys364, Ile365, Asp366, Asn367, Leu368, Phe406 and Val408 corresponding to the $LEDGF_{IBD}$ were among the main residues involved in the interaction with the IN_{CCD} (Figs. 2 and 3 c). The involvement of the above mentioned residues in stabilizing the IN_{CCD}-LEDGF/p75 interaction has also been reported in previous works [33,37].

To compare the structural behavior of the IN_{CCD} and $LEDGF_{IBD}$ in their bound and unbound states, additional 30 ns MD of simulation were obtained for each macromolecule. The flexibility of the previously described hotspots residues was compared by analyzing their *b*-factor values in the bound and unbound proteins (Fig. S1). Notably, two residues from the IN_{CCD} exhibited considerably higher *b*-factor values in the unbound state, namely Glu170A and Trp131B. It is noteworthy that these two residues established the main stabilizing interactions as shown in Fig. 3a and b. In the case of Glu170A, this residue may be crucial for the long-range recognition of the $LEDGF_{IBD}$, and as such constitutes a critical interaction hotspot for the development of potent LEDGINs. In addition, Trp131B is mainly involved in hydrophobic interactions, and its contribution to the complex stabilization is elicited at shorter distances upon IN-LEDGF/p75 binding to the IN_{CCD} interface domain. The rest of the hotspots residues from monomers A and B of the IN_{CCD} exhibited no significant difference in their *b*-factor values between the bound and unbound states, suggesting that the IN_{CCD} is considerably pre-organized for the binding of the $LEDGF_{IBD}$ and that no further induced fitting is required.

When the *b*-factor values obtained for the $LEDGF_{IBD}$ hotspots were analyzed (Fig. S1), higher values were found for the unbound protein with respect to the bound state for almost all residues, suggesting a considerably induced fitting in this macromolecule chain upon binding to the IN_{CCD}. This feature suggests a potential for LEDGF/p75 binding to multiple targets, which is consistent with the normal biological role of this cofactor protein within the cell [51].

3.2. Structural and energetic analysis of IN_{CCD}-LEDGINs crystallographic complexes

Four crystallographic complexes between IN and LEDGINs (**1-4**, Fig. 4) with reported IC_{50} values were selected as initial models to analyze the key pharmacodynamic features driving LEDGINs bioactivity. Model compounds **1-4** were selected for an initial exhaustive analysis since they were co-crystalized with both IN_{CCD} monomers comprising the LEDGINs binding site, and thus further manipulation of the corresponding structures was not required. The corresponding crystallographic complexes were subjected to MD and binding free energy interaction analysis

The corresponding complexes were subjected to an identical MD protocol as the one applied to study the IN-LEDGF/p75 complex. After stages of minimization, heating and equilibration, 30 ns of MD production trajectory were obtained. Fig. S2 shows the RMSD values of **1-4** throughout the trajectory taking the corresponding crystallographic structure as reference. In all cases, the ligand remained bound within the IN_{CCD} interface, maintaining most of the intermolecular interactions observed in the crystal (Fig. S3-S7).

Among the key intermolecular interactions, it was observed that the carboxylic acid moiety in **1-4** established stable hydrogen bond interactions with the NH group of the backbone of Glu170A, His171A and the side chain of Thr174A. In addition, the NH moiety present in all the ligands established a stable hydrogen bond interaction with the carbonyl backbone of Gln168A. The cyclohexyl and metoxy-phenyl ring present in the ligands are positioned within the IN_{CCD} hydrophobic pocket lined by Leu102B, Thr125B, Ala128B, Ala129B, Trp132B, Thr174A and Met178A. It is noteworthy that only compounds **3** and **4** established stable interactions with Trp131B, which are elicited with the butyl and additional metoxy-phenyl moiety in their structures (Fig. S3, S6 and S7, respectively).

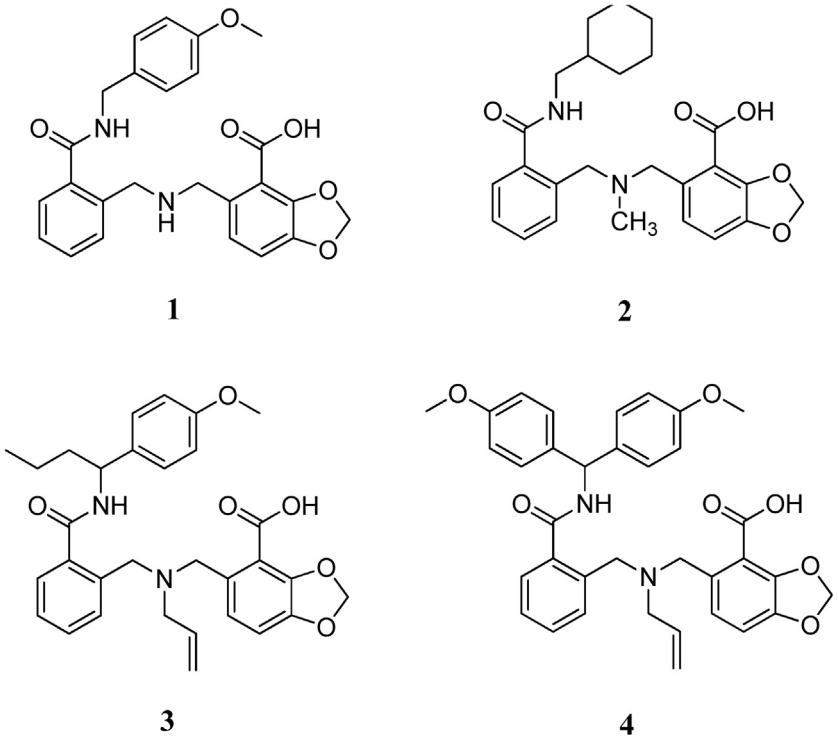

Fig. 4. Molecular structures of LEDGINs **1-4**.

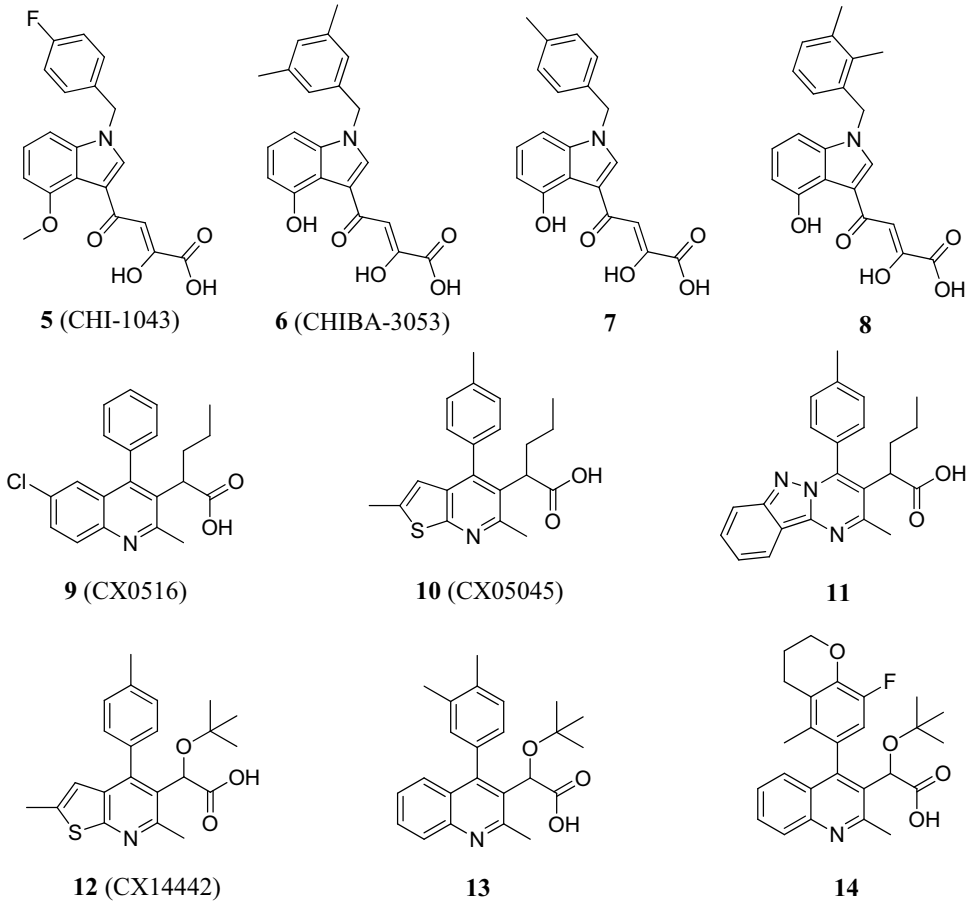

Fig. 5. Molecular structures of LEDGINs **5**-**14**.

Table 1
Energetic components and total interaction energies calculated for the interaction between compounds **1-4** and the IN_{CCD}.

LEDGIN	IC_{50}[a]	pIC_{50}[b]	ELE[c]	VdW[d]	EGB[e]	E_{surf}[f]	ΔG_{bind}[g]
1	270	−2.43	8.37	−36.25	6.85	−4.91	−25.93
2	100	−2.00	8.75	−39.60	−1.80	−4.95	−37.62
3	29	−1.46	−2.98	−39.25	15.18	−5.72	−32.77
4	8.1	−0.91	−22.40	−44.81	37.55	−6.82	−36.48

[a] Half maximal inhibitory concentration (μM).
[b] $-\log IC_{50}$.
[c] Electrostatic contribution.
[d] Van der Waals contribution.
[e] Polar contribution to the solvation free energy.
[f] Non-polar contribution to the solvation free energy.
[g] Total estimated binding free energy interaction.

In a second stage, MMGBSA binding free energy analyses were applied over the MD trajectories with the corresponding binding components being quantified (Table 1).

From these studies, it was found that inhibitory potencies of **1-4** depends on the electrostatic interaction components, with the less potent compounds **1** and **2** exhibiting positive electrostatic interaction magnitudes, while the most potent compounds **3** and **4** exhibited negative electrostatic values. When the binding modes of **1-4** are analyzed in detail, it can be seen that all of them establish hydrogen bond interactions through their carboxyl moiety with the backbone NH group of Glu170A. From the MD trajectories, it was observed that only **3** and **4** were able to maintain a stable interaction that prevents the electrostatic repulsion with the negatively charged side-chain of Glu170A. This repulsion was also described in a previous work [33]. In addition, Van der Waals contributions were significant for all the studied compounds, feature that is also consistent with previous reports [33].

To further analyze the preliminary structure-activity relationship mentioned above, several LEDGINs with reported IC_{50} values and from different structural families were included in our study. Particular emphasis was set in selecting model compounds exhibiting a sub-micromolar IC_{50} value.

3.3. Structural and energetic studies on LEDGINs 5–14

In this stage, ten additional LEDGINs (Fig. 5) were studied to elucidate their intermolecular interaction properties with the IN_{CCD}. Four of them (Fig. 5, **5-8**) belong to the family of substituted N-benzyl-indoles, while the remaining six (Fig. 5, **9-14**) belong to the family of 2-(quinolin-3-yl) acetic acids. Within this new set of model compounds, only **9**, **13** and **14** have been co-crystallized with

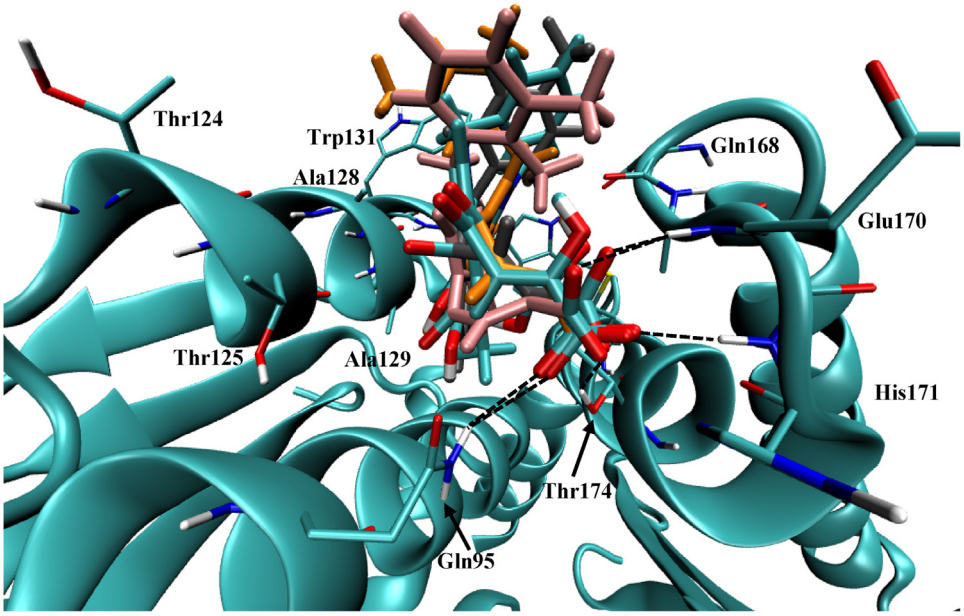

Fig. 6. Binding mode of LEDGINs **5** (cyan), **6** (orange), **7** (grey) and **8** (pink) in complex with the IN_{CCD} obtained from molecular docking studies. Hydrogen bond interactions are shown as cyan lines. (For interpretation of the references to colour in this figure legend, the reader is referred to the web version of this article.)

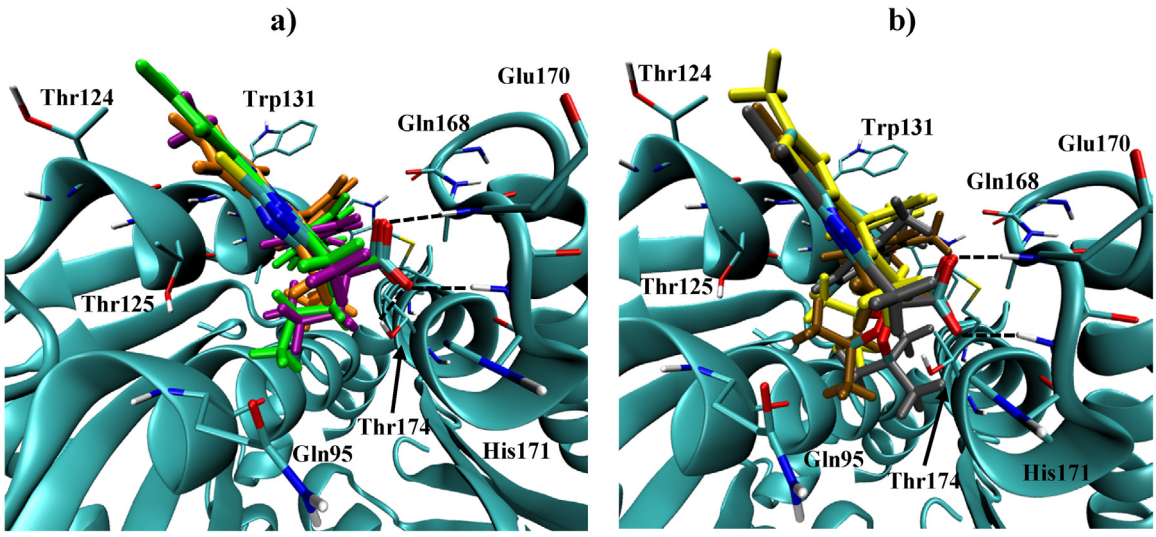

Fig. 7. Binding mode of: a) LEDGINs **9** (orange), **10** (purple) and **11** (green); b) LEDGINs **12** (yellow), **13** (brown) and **14** (grey) in complex with the IN_{CCD} obtained from molecular docking studies. Hydrogen bond interactions are indicated as cyan lines. (For interpretation of the references to colour in this figure legend, the reader is referred to the web version of this article.)

the IN_{CCD} (PDB codes: 3LPU, 4E1M and 4E1N [22,29], respectively) however, only single IN monomers are present in the deposited structures. Consequently, in order to completely model the binding mode of **5-14** to the IN_{CCD}, molecular docking protocols were applied as described in the materials and methods section using the IN_{CCD} corresponding to the crystallographic complex with **4** (PDB code: 3ZSO) as structural template [24]. Fig. 6 presents the three-dimensional binding modes of compounds **5-8** within the IN_{CCD}, while Fig. S8-S11 show the corresponding bidimensional intermolecular interaction plots as obtained for the corresponding docking poses. The resulting intermolecular interaction patterns were similar to those previously reported for compounds **1-4**. In this way, the diketo acid moieties present in **5-8** establish hydrogen bonds interactions with the backbone NH group of Glu170A and His171A and the side chain of Thr174A. The aryl moiety fused to the indole ring interacts with the residues of the IN_{CCD} comprising the hydrophobic pocket, while the N-benzyl substituent interacts with residue Trp131B.

The molecular docking results obtained for **9-14** were also in agreement with the interaction pattern observed for the previously described compounds, and are consistent with previous reports (Fig. 7 and S12-S17) [22,29,33,37]. Again, the carboxylic group established hydrogen bond interactions with the backbone NH group of Glu170A and His171A and with the side chain of Thr174A. The quinolin ring remained exposed to the solvent, while the substituted phenyl ring is oriented towards the interior of the IN_{CCD} hydrophobic pocket. The propyl (**9**-**11**) and *tert*-butyl (**12**-**14**) groups are buried within the cavity lined by residues Gln95B, Thr174A and Leu102 B (Fig. 7 and S12-S17). Remarkably, neither of these compounds established hydrophobic interactions with Trp131B. This feature suggests that the interaction with this residue, which is established in the IN-LEDGF/p75 interaction fin-

Table 2
Energetic components and total interaction energies calculated for the interaction between compounds **5-14** and the IN_{CCD}.

LEDGIN	IC_{50}[a]	pIC_{50}[b]	ELE[c]	VdW[d]	EGB[e]	E_{surf}[f]	ΔG_{bind}[g]
5	36.2	−1.56	−44.59	−32.09	56.99	−5.20	−24.90
6	3.5	−0.54	−64.89	−33.79	73.22	−5.16	−30.60
7	68.0	−1.83	−68.55	−36.56	77.27	−5.23	−33.06
8	28.5	−1.45	−47.54	−36.22	61.37	−5.11	−27.50
9	1.37	−0.14	−66.38	−31.39	70.67	−4.96	−32.06
10	0.58	0.24	−70.72	−34.18	73.31	−5.33	−36.92
11	7.85	−0.89	−76.02	−35.82	79.16	−5.52	−38.18
12	0.046	1.34	−79.38	−37.36	82.48	−5.76	−40.02
13	0.215	0.67	−79.34	−39.20	80.93	−5.18	−42.79
14	0.019	1.72	−82.77	−42.85	87.23	−5.57	−43.96

[a] Half maximal inhibitory concentration (μM).
[b] $-\log IC_{50}$.
[c] Electrostatic contribution.
[d] Van der Waals contribution.
[e] Polar contribution to the solvation free energy.
[f] Non-polar contribution to the solvation free energy.
[g] Total estimated binding free energy interaction.

Table 3
Free energy of binding for the interaction between hotspots residues belonging to the IN_{CCD} and compounds **1-14**.

Hotspot	LEDGIN													
	1	2	3	4	5	6	7	8	9	10	11	12	13	14
Gln168A	−0.361	−1.903	−2.06	−1.422	−0.479	−0.332	−0.302	0.046	−0.072	−0.085	−0.132	−0.138	−0.110	−0.151
Ala169A	−0.972	−4.789	−3.967	−4.721	−1.109	−2.239	−2.765	−0.895	−3.471	−4.039	−3.951	−4.209	−4.266	−4.102
Glu170A	−0.112	−2.301	−2.091	−2.915	−1.244	−1.727	−1.546	−0.736	−3.123	−3.768	−3.674	−3.692	−4.036	−4.029
His171A	−0.207	0.106	−0.048	−0.483	−0.302	−1.212	−0.638	−1.300	−1.406	−2.525	−2.307	−3.012	−3.075	−2.908
Thr174A	−2.009	−1.953	−1.187	−2.296	−0.809	−3.450	−3.009	−1.206	−3.315	−4.079	−4.047	−4.626	−4.382	−4.408
Met178A	−0.974	−0.840	−0.769	−1.078	−0.894	−0.799	−0.763	−0.554	−0.599	−0.606	−0.602	−0.561	−0.705	−0.900
Gln95B	−1.931	−2.954	−4.586	−1.935	−1.349	−2.897	−5.041	−1.446	−0.901	−0.548	−0.502	−0.611	−0.477	−0.524
Thr124B	−0.625	−0.154	−0.358	−0.265	−0.556	−0.179	−0.209	−0.233	−0.412	−0.492	−0.776	−0.306	−0.592	−0.542
Thr125B	−2.041	−1.578	−2.117	−2.283	−1.868	−1.268	−1.646	−2.649	−2.115	−2.646	−2.935	−2.593	−2.740	−2.379
Ala128B	−1.657	−1.467	−2.070	−1.198	−2.446	−2.769	−2.791	−1.246	−1.215	−1.195	−1.523	−1.199	−1.364	−1.829
Ala129B	−1.135	−0.908	−0.888	−0.832	−0.944	−0.694	−0.849	−1.079	−0.694	−0.725	−0.602	−0.650	−0.664	−0.914
Trp131B	−0.282	−0.453	−0.592	−0.832	−0.761	−0.797	−0.945	−0.168	−0.188	−0.089	−0.097	−0.087	−0.127	−0.226
Trp132B	−0.837	−0.861	−1.391	−1.321	−1.344	−1.861	−1.778	−0.701	−0.653	−0.705	−0.707	−0.644	−0.786	−1.386
ΔG_{res}[a]	**−13.14**	**−20.05**	**−19.75**	**−21.58**	**−14.11**	**−20.22**	**−22.28**	**−12.17**	**−18.16**	**−21.50**	**−21.86**	**−22.33**	**−23.32**	**−24.30**

[a] Sum of IN_{CCD} hotspot per-residue decomposition binding free energy interaction.

gerprint (Fig. 3b), is not particularly relevant to attain a potent protein–protein interaction inhibition

As was performed before, the complexes obtained by molecular docking for **9-14** were subjected to MD simulations and binding free energy analyses (Table 2).

Similar to what was observed for **1-4**, the inhibitory potency showed a close correlation with the electrostatic interaction components, with the most potent compounds **12-14** exhibiting the highest intermolecular interaction stabilization represented as a negative electrostatic interaction component. In addition, all the studied compounds exhibited a significant VdW interaction with the IN_{CCD}, as was previously observed for **1-4**. Clearly, the intermolecular interaction is efficiently stabilized by these forces, but biological activity seems not to be driven by this event. A quantitative correlation between the total free energy of binding (ΔG_{bind}) and the inhibitory potency (measured as the pIC_{50}) was explored (Fig. S18), finding a bad correlation.

Our results and previous reports evidence that targeting the IN_{CCD} hotspot residues is critical to obtain a high inhibitory potency [33]. Thus, a per-residue free energy of binding decomposition was performed to assess the contribution of every IN_{CCD} residue to the binding of compounds **1-14** (Table 3).

All the studied compounds displayed favorable interaction with the IN_{CCD} hotspots residues. A new linear correlation between the sum of the interaction energies with the hotspots residues (ΔG_{res}) and the corresponding pIC_{50} values was explored (Fig. S19). Again, a bad correlation was found, still indicating the presence of additional physicochemical features involved in the inhibition of the IN-LEDGF/p75 interaction.

Clearly, besides the binding free energy of interaction parameters, additional structural properties are associated to this PPI inhibition. One possibility is that the structural and energetic requirements to adopt the three-dimensional conformation able to efficiently comply with the hotspots interactions (i.e. bioactive conformation) may also drive the inhibitory potency, feature that may be biased in a typical molecular docking study. To assess this possibility, exhaustive molecular docking assays were further performed starting from conformer libraries obtained at energy barriers of increasing values.

3.4. Search for the bioactive conformation

In the search for additional physicochemical properties driving the inhibitory potency of **1-14**, an exhaustive conformational search was performed prior to molecular docking studies. Conformer libraries of the ligands were systematically obtained within 1–70 Kcal/mol at a 1 Kcal/mol step. The corresponding libraries were afterwards redocked to the IN_{CCD} following identical protocols as those reported before. The presence of the bioactive conformation within the corresponding library of conformers was confirmed by measuring the resulting RMSD values of the lowest docked energy conformation using as reference the ligand-IN_{CCD} described in the previous section. A positive hit was considered when the resulting RMSD values were below 1 Å. As a result of

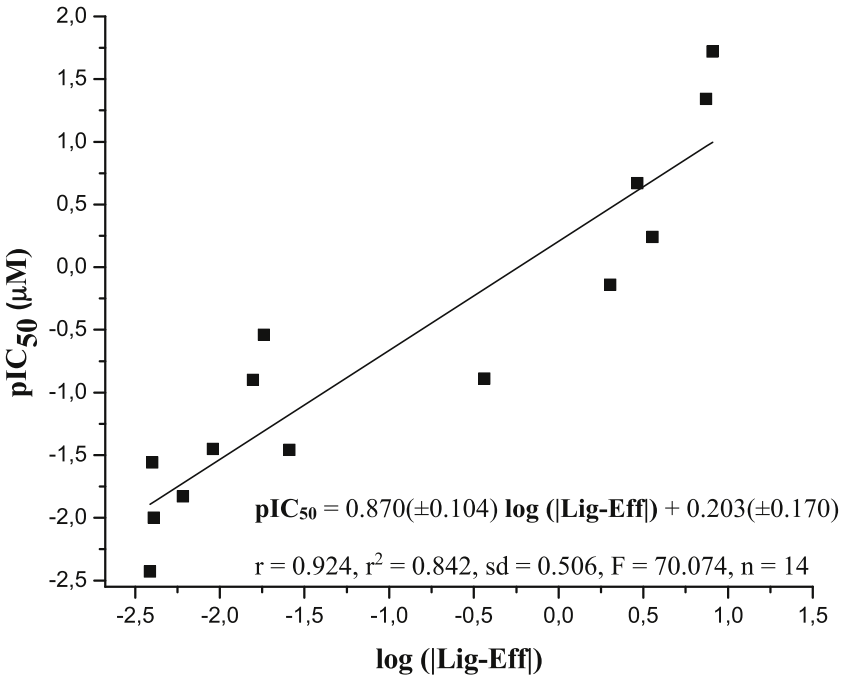

Fig. 8. Linear correlation between LEDGINs (**1-14**) biological activity (pIC_{50}) and the log(|Lig-Eff|) as determined in this work.

Table 4
Results obtained from the systematic conformational analysis of LEDGINs **1-14**.

LEDGIN	Confs[a]	EB[b]	|Lig-Eff|[c]
1	3386	4	0.004
2	4907	10	0.002
3	765	5	0.025
4	1375	6	0.016
5	3528	10	0.004
6	1109	8	0.018
7	3682	18	0.006
8	1335	8	0.009
9	9	17	2.008
10	6	13	3.570
11	60	61	0.363
12	3	11	7.412
13	8	13	2.904
14	3	15	8.063

[a] *Confs*: Number of conformers present in the library containing the corresponding bioactive conformation.
[b] *EB*: lowest energetic barrier (Kcal/mol) at which the bioactive conformation was found.
[c] |*Lig-Eff*|: Ratio between the ΔG_{res} and the number of conformers present on the conformers library with the bioactive conformation.

this search, both the energy barrier and the number of conformers present in the library containing the bioactive conformations were tabulated (Table 4). From these results, a "ligand efficiency" (**|Lig-Eff|**) factor was calculated as the absolute value of the ratio between the ΔG_{res} and the number of conformers present in the library containing the bioactive conformation.

As can be seen, compounds **1-8** exhibit a significantly higher flexibility than compounds **9-14**. It is noteworthy that compounds **12-14** displayed the lowest number of conformers, feature that is originated by the steric hindering effect elicited by the *tert*-butyl moieties present in their structure (**12-14**).

The quantitative relationship between the logarithm of the |Lig-Eff| parameter and the pIC_{50} is shown in Fig. 8. As can be seen a very good correlation was found, evidencing that, in addition to an efficient interaction with the binding site hotspots, the molecular flexibility and structural pre-organization of the corresponding LEDGIN constitute a critical feature for the potent inhibition of the IN-LEDGF/p75 interaction.

4. Conclusions

In this work, state of the art structure-based drug design strategies, including molecular docking, MD simulations and binding free energy analyses were used to develop a quantitative relationship between the binding efficiency and the inhibitory potency of a set of 14 LEDGINs. Our contribution to the research field involves an exhaustive exploration of the critical PPI hotspots required for an efficient inhibition of the IN-LEDGF/p75 interaction. We also demonstrated that in addition to the pharmacodynamic requirements involved in the interaction with the receptor, a high preorganization state of the ligand in the corresponding bioactive conformation confers a significantly higher inhibitory potency, and is typically required to attain a sub micromolar IC_{50} values. To the best of our knowledge, this is the first report presenting a very good correlation between the binding efficiency of LEDGINs to the IN_{CCD} and their corresponding IN-LEDGF/p75 interaction inhibitory potency. The conclusions raised in this work may constitute a significant aid in the search of new LEDGINs with optimized interaction and conformational properties that may exhibit sub micromolar inhibitory activity.

Acknowledgments

The authors gratefully acknowledge financial support from the Secretaria de Ciencia y Técnica of the Universidad Nacional de Córdoba (SECYT-UNC), the Consejo Nacional de Investigaciones Científicas y Técnicas (CONICET) and the Agencia Nacional de Promoción Científica y Técnica (ANPCyT), Argentina. Sergio R. Ribone also acknowledges postdoctoral fellowship from CONICET. Authors also acknowledges the GPGPU Computing Group from the Facultad de Matemática, Astronomía y Física (FAMAF), Universidad Nacional de Córdoba, Argentina, for providing access to computing resources.

Appendix A. Supplementary data

Supplementary data associated with this article can be found, in the online version, at http://dx.doi.org/10.1016/j.jmgm.2017.05.019.

References

[1] R. Di Santo, Inhibiting the HIV Integration Process: Past, Present, and the Future, J. Med. Chem. 57 (2013) 539–566.
[2] Y. Li, S. Xuan, Y. Feng, A. Yan, Targeting HIV-1 integrase with strand transfer inhibitors, Drug Discov. Today 20 (2015) 435–449.
[3] S.X. Gu, P. Xue, X.L. Ju, Y. Zhu, Advances in rationally designed dual inhibitors of HIV-1 reverse transcriptase and integrase, Bioorg. Med. Chem. 24 (2016) 5007–5016.
[4] B.Y.T. Nguyen, R.D. Isaacs, H. Teppler, R.Y. Leavitt, P. Sklar, M. Iwamoto, L.A. Wenning, M.D. Miller, J. Chen, R. Kemp, W. Xu, R.A. Fromtling, J.P. Vacca, S.D. Young, M. Rowley, M.W. Lower, K.M. Gottesdiener, D.J. Hazuda, Raltegravir: the first HIV-1 integrase strand transfer inhibitor in the HIV armamentarium, Ann. N. Y. Acad. Sci. 3 (2011) 83–89.
[5] J.L. Blanco Arévalo, G.G. Whitlock, Dolutegravir An exciting new kid on the block, Expert Opin. Pharmacother. 15 (2014) 573–582.
[6] T. Wills, V. Vega, Elvitegravir: a once-daily inhibitor of HIV-1 integrase, Expert Opin. Investig. Drugs 21 (2012) 395–401.
[7] L.Q. Al-Mawsawi, N. Neamati, Allosteric inhibitor development targeting HIV-1 integrase, ChemMedChem 6 (2011) 228–241.
[8] P. Zhan, C. Pannecouque, E. De Clercq, X. Liu, Anti-HIV drug discovery and development: current innovations and future trends, J. Med. Chem. 59 (2016) 2849–2878.
[9] B. Van Maele, K. Busschots, L. Vandekerckhove, F. Christ, Z. Debyser, Cellular co-factors of HIV-1 integration, Trends Biochem. Sci. 31 (2006) 98–105.
[10] M. Llano, D.T. Saenz, A. Meehan, P. Wongthida, M. Peretz, W.H. Walker, W. Teo, E.M. Poeschla, An essential role for LEDGF/p75 in HIV integration, Science 314 (2006) 461–464.
[11] Z. Debyser, B.A. Desimmie, O. Taltynov, J. Demeulemeester, F. Christ, Validation of host factors of HIV integration as novel drug targets for anti-HIV therapy, MedChemComm 5 (2014) 314–320.
[12] A. Engelman, J.J. Kessl, M. Kvaratskhelia, Allosteric inhibition of HIV-1 integrase activity, Curr. Opin. Chem. Biol. 17 (2013) 339–345.
[13] J.A. Wells, C.L. McClendon, Reaching for high-hanging fruit in drug discovery at protein–protein interfaces, Nature 450 (2007) 1001–1009.
[14] M.R. Arkin, J.A. Wells, Small-molecule inhibitors of protein–protein interactions: progressing towards the dream, Nat. Rev. Drug Discov. 3 (2004) 301–317.
[15] W. Guo, J.A. Wisniewski, H. Ji, Hot spot-based design of small-molecule inhibitors for protein?protein interactions, Bioorg. Med. Chem. Lett. 24 (2014) 2546–2554.
[16] A. Voet, E.F. Banwell, K.K. Sahu, J.G. Heddle, K.Y.J. Zhang, Protein interface pharmacophore mapping tools for small molecule protein: protein interaction inhibitor discovery, Curr. Top. Med. Chem. 13 (2013) 989–1001.
[17] P. Cherepanov, A.L.B. Ambrosio, S. Rahman, T. Ellenberger, A. Engelman, Structural basis for the recognition between HIV-1 integrase and transcriptional coactivator p75, Proc. Natl. Acad. Sci. U. S. A. 102 (2005) 17308–17313.
[18] P. Cherepanov, E. Devroe, P.A. Silver, A. Engelman, Identification of an evolutionarily conserved domain in human lens epithelium-derived growth factor/transcriptional co-activator p75 (LEDGF/p75) that binds HIV-1 integrase, J. Biol. Chem. 279 (2004) 48883–48892.
[19] P. Cherepanov, Z.Y.J. Sun, S. Rahman, G. Maertens, G. Wagner, A. Engelman, Solution structure of the HIV-1 integrase-binding domain in LEDGF/p75, Nat. Struct. Mol. Biol. 12 (2005) 526–532.
[20] K. Busschots, A. Voet, M. De Maeyer, J.C. Rain, S. Emiliani, R. Benarous, L. Desender, Z. Debyser, F. Christ, Identification of the LEDGF/p75 binding site in HIV-1 integrase, J. Mol. Biol. 365 (2007) 1480–1492.
[21] S. Hare, P. Cherepanov, The interaction between lentiviral integrase and LEDGF: Structural and functional insights, Viruses 1 (2009) 780–801.
[22] F. Christ, A. Voet, A. Marchand, S. Nicolet, B.A. Desimmie, D. Marchand, D. Bardiot, N.J. Van Der Veken, B. Van Remoortel, S.V. Strelkov, M. De Maeyer, P. Chaltin, Z. Debyser, Rational design of small-molecule inhibitors of the LEDGF/p75-integrase interaction and HIV replication, Nat. Chem. Biol. 6 (2010) 442–448.
[23] J. Demeulemeester, C. Tintori, M. Botta, Z. Debyser, F. Christ, Development of an AlphaScreen-based HIV-1 integrase dimerization assay for discovery of novel allosteric inhibitors, J. Biomol. Screen 17 (2012) 618–628.
[24] T.S. Peat, D.I. Rhodes, N. Vandegraaff, G. Le, J.A. Smith, L.J. Clark, E.D. Jones, J.A.V. Coates, N. Thienthong, J. Newman, O. Dolezal, R. Mulder, J.H. Ryan, G.P. Savage, C.L. Francis, J.J. Deadman, Small molecule inhibitors of the LEDGF site of human immunodeficiency virus integrase identified by fragment screening and structure based design, PLoS One 7 (2012) e40147.
[25] L. De Luca, S. Ferro, R. Gitto, M.L. Barreca, S. Agnello, F. Christ, Z. Debyser, A. Chimirri, Small molecules targeting the interaction between HIV-1 integrase and LEDGF/p75 cofactor, Bioorg. Med. Chem. 18 (2010) 7515–7521.
[26] F. Christ, S. Shaw, J. Demeulemeester, B.A. Desimmie, A. Marchan, S. Butler, W. Smets, P. Chaltin, M. Westby, Z. Debyser, C. Pickford, Small-molecule inhibitors of the LEDGF/p75 binding site of integrase block HIV replication and modulate integrase multimerization, Antimicrob. Agents Chemother. 56 (2012) 4365–4374.
[27] E. Serrao, B. Debnath, H. Otake, Y. Kuang, F. Christ, Z. Debyser, N. Neamati, Fragment-based discovery of 8-hydroxyquinoline inhibitors of the HIV-1 integrase-lens epithelium-derived growth factor/p75 (IN-LEDGF/p75) interaction, J. Med. Chem. 56 (2013) 2311–2322.
[28] T.W. Sanchez, B. Debnath, F. Christ, H. Otake, Z. Debyser, N. Neamati, Discovery of novel inhibitors of LEDGF/p75-IN protein–protein interactions, Bioorg. Med. Chem. 21 (2013) 957–963.
[29] M. Tsiang, G.S. Jones, A. Niedziela-Majka, E. Kan, E.B. Lansdon, W. Huang, M. Hung, D. Samuel, N. Novikov, Y. Xu, M. Mitchell, H. Guo, K. Babaoglu, X. Liu, R. Geleziunas, R. Sakowicz, New class of HIV-1 integrase (IN) inhibitors with a dual mode of action, J. Biol. Chem. 287 (2012) 21189–21203.
[30] Y. Zhao, Z. Luo, Recent advances in the development of small-molecular inhibitors target HIV integrase-LEDGF/p75 interaction, Mini Rev. Med. Chem. 15 (2015) 1195–1208.
[31] J. Demeulemeester, M. De Maeyer, Z. Debyser, HIV-1 integrase drug discovery comes of age, in: W.E. Diederich, H. Steuber (Eds.), Topics in Medicinal Chemistry, vol. 15, Springer, 2015, pp. 1–15.
[32] J. Demeulemeester, P. Chaltin, A. Marchand, M. De Maeyer, Z. Debyser, F. Christ, LEDGINs:non-catalytic site inhibitors of HIV-1 integrase: a patent review (2006–2014), Expert Opin. Ther. Pat. 24 (2014) 609–632.
[33] L. De Luca, F. Morreale, A. Chimirri, Insight into the fundamental interactions between LEDGF binding site inhibitors and integrase combining docking and molecular dynamics simulations, J. Chem. Inf. Model. 52 (2012) 3245–3254.
[34] L. De Luca, F. Morreale, F. Christ, Z. Debyser, S. Ferro, R. Gitto, New scaffolds of natural origin as Integrase–LEDGF/p75 interaction inhibitors: virtual screening and activity assays, Eur. J. Med. Chem. 68 (2013) 405–411.
[35] L. De Luca, S. Ferro, F. Morreale, A. Chimirri, Inhibition of the interaction between HIV-1 integrase and its cofactor LEDGF/p75: a promising approach in anti-retroviral therapy, Mini Rev. Med. Chem. 11 (2011) 714–727.
[36] G. Hu, X. Li, X. Zhang, Y. Li, L. Ma, L.M. Yang, G. Liu, W. Li, J. Huang, X. Shen, L. Hu, Y.T. Zheng, Y. Tang, Discovery of inhibitors to block interactions of HIV-1 integrase with human LEDGF/p75 via structure-based virtual screening and bioassays, J. Med. Chem. 55 (2012) 10108–10117.
[37] W. Xue, H. Liu, X. Yao, Molecular modeling study on the allosteric inhibition mechanism of HIV-1 integrase by LEDGF/p75 binding site inhibitors, PLoS One 9 (2014) e87077.
[38] C. Zardecki, S. Dutta, D.S. Goodsell, M. Voigt, S.K. Burley, RCSB protein data bank: a resource for ChemicalBiochemical, and structural explorations of large and small biomolecules, J. Chem. Educ. 93 (2016) 569–575.
[39] Fred.3.0.0 OpenEye Scientific Software, S. F., NM http://www.eyesopen.com.
[40] Omega.2.4.3.tific.Software. OpenEye Scientific Software.
[41] OpenEye.Scientific.Software. OpenEye Scientific Software.
[42] VIDA.4.2.1. OpenEye Scientific Software, Santa Fe, NM http://www.eyesopen.com.
[43] D.A. Case, J.T. Berryman, R.M. Betz, D.S. Cerutti, T.E. Cheatham III, T.A. Darden, R.E. Duke, T.J. Giese, H. Gohlke, A.W. Goetz, N. Homeyer, S. Izadi, P. Janowski, J. Kaus, A. Kovalenko, T.S. Lee, S. LeGrand, P. Li, T. Luchko, R. Luo, B. Madej, K.M. Merz, G. Monard, P. Needham, H. Nguyen, H.T. Nguyen, I. Omelyan, A. Onufriev, D.R. Roe, A.E. Roitberg, R. Salomon-Ferrer, C. Simmerling, W. Smith, J. Swails, R.C. Walker, J. Wang, R.M. Wolf, X. Wu, D.M. York, P.A. Kollman, Amber 14, University of California, San Francisco, 2014.
[44] M.J. Frisch, G.W. Trucks, H.B. Schlegel, G.E. Scuseria, M.A. Rob, J.R. Cheeseman, J.A. Montgomery Jr., T. Vreven, K.N. Kudin, J.C. Burant, J.M. Millam, S.S. Iyengar, J. Tomasi, V. Barone, B. Mennucci, M. Cossi, G. Scalmani, N. Rega, G.A. Petersson, H. Nakatsuji, M. Hada, M. Ehara, K. Toyota, R. Fukuda, J. Hasegawa, M. Ishida, T. Nakajima, Y. Honda, O. Kitao, H. Nakai, M. Klene, X. Li, J.E. Knox, H.P. Hratchian, J.B. Cross, V. Bakken, C. Adamo, J. Jaramillo, R. Gomperts, R.E. Stratmann, O. Yazyev, A.J. Austin, R. Cammi, C. Pomelli, J.W. Ochterski, P.Y. Ayala, K. Morokuma, G.A. Voth, P. Salvador, P.J.J. Dannenberg, V.G. Zakrzewski, S. Dapprich, A.D. Daniels, M.C. Strain, O. Farkas, M.A. Al-Laham, C.Y. Peng, A. Nanayakkara, M. Challacombe, P.M.W. Gill, B. Johnson, W. Chen, M.W. Wong, C. Gonzalez, J.A. Pople, Gaussian03, Gaussian Inc., Pittsburgh, PA, 2003.
[45] J. Wang, R.M. Wolf, J.W. Caldwell, P.A. Kollman, D.A. Case, Development and testing of a general amber force field, J. Comput. Chem. 25 (2004) 1157–1174.
[46] J.A. Maier, C. Martinez, K. Kasavajhala, L. Wickstrom, K.E. Hauser, C. Simmerling, ff14SB: improving the accuracy of protein side chain and backbone parameters from ff99SB, J. Chem. Theor. Comput. 11 (2015) 3696–3713.
[47] B.R. Miller, T.D. McGee, J.M. Swails, N. Homeyer, H. Gohlke, A.E. Roitberg, MMPBSA.py: an efficient program for end-state free energy calculations, J. Chem. Theor. Comput. 8 (2012) 3314–3321.
[48] P.A. Kollman, I. Massova, C. Reyes, B. Kuhn, S. Huo, L. Chong, M. Lee, T. Lee, Y. Duan, W. Wang, O. Donini, P. Cieplak, J. Srinivasan, D.A. Case, T.E. Cheatham III, Calculating structures and free energies of complex molecules: combining molecular mechanics and continuum models, Acc. Chem. Res. 33 (2000) 889–897.
[49] M.J. Vainio, J.S. Puranen, M.S. Johnson, ShaEP: molecular overlay based on shape and electrostatic potential, J. Chem. Inf. Model. 49 (2009) 492–502.
[50] N.M. O'Boyle, M. Banck, C.A. James, C. Morley, T. Vandermeersch, G.R. Hutchison, Open babel: an open chemical toolbox, J. Cheminf. 3 (2011).
[51] M. Llano, J. Morrison, E.M. Poeschla, Virological and cellular roles of the transcriptional coactivator LEDGF/p75, Curr. Top. Microbiol. Immunol. 339 (2009) 125–146.